Copy No. 32

NASA PROGRAM GEMINI WORKING PAPER NO. 5034

LANDING DYNAMICS TEST OF A $\frac{1}{3}$-SCALE PARA-SAIL/LANDING-ROCKET MODEL

NATIONAL AERONAUTICS AND SPACE ADMINISTRATION

MANNED SPACECRAFT CENTER

HOUSTON, TEXAS

August 11, 1965

(NASA-TM-X-69858) LANDING DYNAMICS TEST OF A 1/3-SCALE PARA-SAIL/LANDING-ROCKET MODEL (NASA) 33 p

N74-70729

Unclas

00/99 16446

NASA PROGRAM GEMINI WORKING PAPER NO. 5034

LANDING DYNAMICS TEST OF A $\frac{1}{3}$-SCALE PARA-SAIL/LANDING-ROCKET MODEL

Prepared by: Jerry E. McCullough

Jerry E. McCullough
AST, Landing Dynamics Section

Harold E. Benson

Harold E. Benson
Head, Landing Dynamics Section

Authorized for Distribution:

Warren Gillespie, Jr.

for Maxime A. Faget
Assistant Director for Engineering and Development

NATIONAL AERONAUTICS AND SPACE ADMINISTRATION
MANNED SPACECRAFT CENTER
HOUSTON, TEXAS

August 11, 1965

CONTENTS

TABLES

FIGURES

LANDING DYNAMICS TEST OF A $\frac{1}{3}$-SCALE PARA-SAIL/LANDING-ROCKET MODEL

By J. E. McCullough and H. E. Benson

SUMMARY

Investigations of a $\frac{1}{3}$-scale Gemini model were conducted to determine the feasibility of using the Para-Sail/landing-rocket combination as the landing system on the present Gemini spacecraft. The model used in these tests was a dynamically scaled Gemini configuration which incorporated a cold-gas retrorocket deceleration system and a tricycle-skid landing gear.

A high-pressure nitrogen system was used in the model to simulate the thrust-time curve of a solid-propellant retrorocket, and the full-size landing gear was simulated in the model with respect to the force-stroke curve of the energy absorber.

Instrumentation of the model included accelerometers on the vehicle's three axes to record impact accelerations and the necessary pressure transducers to determine the performance of the cold-gas landing-rocket systems. In addition, high-speed motion pictures were made of each test.

This test series consisted of impacting the model at simulated horizontal velocities of 0, 15, 30, and 50 ft/sec with a simulated vertical impact velocity of 10 ft/sec. Also, one test was conducted with the vehicle landing backwards at a horizontal velocity of 10 ft/sec. The model's pitch attitude was varied $\pm 5^\circ$ from the nominal design of -13°, and the model was yawed in increments of 5° to a maximum of 15°.

Recorded impact accelerations were low, with a maximum of 7.4g occurring parallel to the model's Y-axis. The other two accelerometers recorded 3.65g or less.

The results of these landing tests indicate that the Gemini spacecraft is capable of making safe aircraft-type landings on flat, smooth, compact terrain through this complete range of test conditions with the exception of backward horizontal velocities.

In the presence of irregular or soft landing surfaces where skid penetration or tripping occurs, the vehicle will tumble. Also, landing gear failure is probable in the event of extreme yaw or negative (backward) velocity conditions.

INTRODUCTION

The Gemini spacecraft, unlike its predecessor Mercury, had as an original requirement that it be recovered with no damage that would prevent its reuse. This design goal led to the adoption of the paraglider-tricycle-skid landing system. In the event that any of the stages in development of the paraglider system should become insurmountable in the time available, a possible alternate recovery system was conceived. This was the Para-Sail/landing-rocket system.

The design philosophy for incorporating the Para-Sail/landing-rocket system into the Gemini spacecraft was based on a minimum modification to the existing Gemini spacecraft. With this approach, it was agreed to retain the present tricycle-skid landing gear. The location of the rocket motors in the vehicle was also based on a minimum modification with due consideration to the attitude of the vehicle during descent.

This report presents a discussion of the design of the Para-Sail/landing-rocket landing system for the Gemini spacecraft, and the test results from a $\frac{1}{3}$-scale Para-Sail/landing-rocket model which was impacted on three types of landing surfaces.

GEMINI LANDING ROCKET SYSTEM DESIGN

In order to retain the present Gemini tricycle-skid landing gear in the Para-Sail/landing-rocket system, the attitude of the vehicle at touchdown must remain essentially the same as that for the paraglider system. With this constraint and with the design philosophy of minimum modification, the landing rockets are located in the lower equipment bay of the Gemini vehicle. Photographs of the full-scale and $\frac{1}{3}$-scale landing system are shown in figure 1.

The performance requirements for the solid-propellant rocket motor were chosen to decrease the terminal vertical velocity of the vehicle descending on the Para-Sail parachute from 30 ft/sec to 10 ft/sec or less. The length and depth of the center equipment bay dictates the use of a pair of rocket motors to achieve the desired performance. The motors are rolled 6.5° about their longitudinal axis to enable the thrust vector for each motor to pass through the nominal center-of-gravity of the vehicle. The location also dictates that the thrust vector be perpendicular to the longitudinal centerline of the motor. The boost thrust level is 5950 pounds thrust for 0.4 second and the sustain thrust level is 1220 pounds thrust for 1.1 second for each motor. One or more probes will be used to sense the correct altitude for igniting the rocket motors.

MODEL DESCRIPTION

The Para-Sail has lower horizontal and higher vertical velocities than the paraglider; therefore, it became necessary to study and test the present Gemini configuration to determine how these changes in velocities affect landing impact and stability of the vehicle. Prior to any full-scale testing of such a system, a $\frac{1}{3}$-scale model test program was initiated. The specific objectives of this program were to determine the accelerations during impact and the stability characteristics of the Gemini vehicle under simulated Para-Sail/landing rocket landing conditions. This program was designed to establish critical test parameters, to furnish design data, to verify design, and to obtain test data prior to full-scale testing.

The model used for these tests was a $\frac{1}{3}$-dynamically-scaled model of the Gemini spacecraft. The model's overall dimensions, center-of-gravity, location, weight, and moments of inertia shown in figure 2 are proportional to the Gemini spacecraft. The Gemini landing gear and shock absorbers were simulated both in size and action. Tapered aluminum honeycomb was used in the shock attenuators as the energy absorbing material. An effort was made to duplicate the load-stroke curve of the Gemini shock attenuators, as furnished by McDonnell Aircraft Corporation. Photographs of the landing gear and shock attenuators are included in figures 3 to 5.

The model parameters were obtained by scaling the prototype parameters. The only prototype parameter that could not easily be simulated was the drag force of the parachute. Therefore, the effect of the parachute drag force was compensated for in the model program by adjusting the initial velocity of the model using the equations of motion. However, it should be emphasized that all other parameters were scaled, including the model velocity, at the instant of boost-phase thrust. The following scale factors are applicable:

Quantity	Full size	Scale factor	Model
Length	l	y	yl
Time	t	$\sqrt{y}$	$\sqrt{y}\,t$
Mass	m	y^3	y^3m
Weight	w	y^3	y^3w
Acceleration	a	1	a
Coefficient of friction	u	1	u
Force	F	y^3	y^3F
Velocity	V	$\sqrt{y}$	$\sqrt{y}\,V$
Moment of inertia	I	y^5	y^5I

For the model used in the test, y was chosen as $\frac{1}{3}$.

The propulsion system used to simulate the solid propellant rocket motors used compressed nitrogen gas, expanding from a common manifold through two nozzles. The propulsion system is shown schematically in figure 6. The nitrogen gas was stored in the tanks at a pressure of 3000 psi and was regulated to the pressure required at the nozzle to produce the desired thrust. The two nozzles, mounted in the manifold, were run on a thrust stand to obtain the net resultant thrust as a function of nozzle pressure. The boost thrust level was governed by the regulator dome pressure setting. In order to obtain the sustain thrust, it was necessary to reduce the regulator dome pressure. This was achieved by opening the regulator dome solenoid valve momentarily to allow the regulator dome pressure to decrease to the desired value.

In order to control the system, an electronic sequencer was used to control the time intervals within a few milliseconds. The sequencer contained two R-C network channels, one for opening and closing the regulator dome solenoid valve and one for opening and closing the nozzle solenoid valve. A start signal was fed into the sequencer by the closing of a microswitch when the model physically separated from the drop tower. This start signal initiated both R-C networks; however, both the bandwidth and the total time for each R-C network were controlled individually by variable potentiometers.

Reference 1 presents a complete discussion of the full-scale solid propellant motors and the cold-gas system used in these tests.

TEST PROCEDURE

The model was suspended from the compound pendulum carriage (figs. 7 and 8), and its vertical height above the impact surface was adjusted for a calculated vertical velocity. The pendulum was then pulled back by a cable winch to a specific height so that its horizontal component of velocity was also established. The supporting carriage fixture was adjustable so that the model could be given any desired initial pitch and yaw attitude. Because of the nature of the pendulum, the model retained the initial pitch throughout the swing. On release, the pendulum swung through its arc and actuated a microswitch which, in turn, caused the attachment mechanism to release the model at the neutral position on the pendulum's swing arc. The model then impacted and slid to a stop on the prepared surfaces without any restraint except its trailing umbilical cable. To neutralize this effect as much as possible, the cable was given an initial horizontal velocity equal to that of the model.

Onboard instrumentation consisted of four strain-gage accelerometers and two pressure transducers. Three accelerometers were installed at the model's center of gravity along the three principle axes to record impact accelerations. Another accelerometer was mounted at the nozzle manifold to record accelerations along the thrust axis. The pressure transducers were installed so that nozzle pressures were recorded. Output signals from these instruments were transmitted through an umbilical cable to the amplifying and recording equipment.

Model impact attitudes, in addition to motions and displacements which occurred after contact, were recorded by three stationary 16-mm high-speed motion-picture cameras.

MODEL TEST

Tests were made in two general phases. In the first, without using the propulsion system, the model was tested on two types of possible landing terrains, and it was assumed that the rockets had performed under nominal conditions. In the second phase, the propulsion system was employed as an active system.

Phase I - Impact Test on Sod and Soil

In phase I, two types of landing surfaces were used to determine to what degree terrain conditions affect stability. The propulsion system was not used, and the model was dropped at velocities that would be present if the rocket motors had fired under normal conditions.

Tests 1 to 11 were conducted on a landing surface prepared by covering hard-packed soil with a mat of St. Augustine grass composed of 1-foot square sections of sod placed close together. To fix the sod squares rigidly into a reasonably uniform surface and to prevent the squares from slipping, loose sand was packed between them. For tests 12 to 24, the sod and sand were removed, and the hard-packed soil was leveled to remove surface irregularities.

Before testing on each of the two surfaces, data were recorded to permit calculation of coefficients of friction, penetration, and relative roughness. To obtain the coefficient of friction, the force required to slide the model over the surface was recorded with a load cell. The coefficient of friction was calculated to be 0.49 for the sod surface and 0.50 for the hard-packed soil.

The relative hardness of the impact surfaces was obtained by dropping a sphere, which measured 5 inches in diameter and weighed 16 pounds, from a height of 7 feet and measuring the depth of impact impression. The sphere was dropped 10 times on each of the two surfaces, and the average depressions were calculated. The average depressions were calculated to be 1.44 and 1.38 inches for the sod and the compacted soil, respectively.

The average difference in ground elevation was 0.3 inch every 2 feet, with a maximum difference of 1.0 inch per 2 feet for the sod surface. No attempt was made to calculate the relative roughness of the soil because the surface was leveled by dragging prior to testing. Throughout these tests the pitch and vertical velocity were maintained at a constant -13° (nose-down attitude) and 10 ft/sec (full-scale), respectively. The yaw angle was varied in increments of 5° from 0° to 15° for each of the horizontal velocities of 0, 15, 30, and 50 ft/sec. In addition, one test was made landing the model backwards (180° yaw) at 10 ft/sec (full-scale) horizontal velocity.

Phase II - Impact Tests on Canvas with Active Propulsion System

The conditions for the phase II, tests 25 to 50, were basically the same as those for the first phase, except that an active propulsion system was used. The purpose of phase II was to verify the results of the phase I in which impact conditions were based on assumptions that the propulsion system had performed properly. Also, phase II investigated the effect of the rockets' sustainer thrust on the vehicular stability during slide-out.

The landing surface for phase II was the smooth, compacted soil covered with canvas tarps to reduce the amount of dust activated by the rocket blast. The coefficient of friction for the canvas was calculated to be 0.42 by using data taken prior to rocket thrust. A second coefficient of friction obtained during employment of the propulsion system was calculated to be 0.55. It is believed that this higher coefficient can be attributed to removal of dust from the surface of the canvas by the rocket exhaust.

The model was dropped from a predetermined height and allowed to fall free until the desired initial velocity was achieved. The sequencer was preset so that approximately 90 percent of boost thrust was achieved at the instant the desired initial velocity was reached. The sequencer was also preset to allow the proper time interval for the boost and sustain thrust phases.

The nominal initial vertical velocity for this test series was constant at 14.3 ft/sec. The only variations in initial vertical velocity were due to variations in the sequencer and the response of the propulsion system. The horizontal velocities tested were 0, 15, 22.5, and 30 ft/sec. The pitch angle was varied from a nominal of -13° (nose down) to $\pm5^\circ$. The yaw angle was varied in increments of 5° from 0° to 15°. Tests were performed with combinations of these horizontal velocities and pitch and yaw angles.

One additional test was conducted with the canvas tarps removed. In this test the model was pulled along with an average horizontal velocity of 3.5 ft/sec, with the retrorockets thrusting at the sustainer level. The purpose of this test was to obtain preliminary data on the amount of soil erosion resulting from the rocket thrust.

RESULTS AND DISCUSSION

The general landing behavior was similar for all conditions. It was characterized by an approach at the predetermined attitude, impact on the main gear, angular rotation until nose gear impact, and by the slide-out. On initial contact of the main skids, a portion of the sink speed energy was absorbed by the rear shock attenuators, and the vehicle was given a rotational impulse in pitch. The resulting vertical and rotational energy in the system was then absorbed during primary nose gear impact, by both the nose and main gear energy absorbers. Energy due to the horizontal landing velocity was largely dissipated by skid friction forces during slide-out, and by the resistance force of the skids riding over or shearing the impact indentations in the landing surface.

During yawed landings without the propulsion system, the vehicle returned to an approximately unyawed slide-out position during the time between the initial impact of the main and nose gears.

Stability on Sod and Soil Surfaces Without Propulsion

In all tests on the sod surface where the horizontal velocity and yaw angle did not exceed 30 ft/sec and 0°, respectively, the model appeared dynamically stable. However, a horizontal velocity of 30 ft/sec combined with a yaw angle of 5° caused the nose skid drag force to become large enough that the model turned over or rolled slowly over in the direction of travel. This tendency recurred at 30-ft/sec horizontal velocity and 10° yaw; therefore, tests were not made at greater yaw angles.

Tumbling also occurred at 50-ft/sec horizontal velocity and 0° yaw. This was a violent end-over-end motion in which the model nose skid dug into the turf, pitched 360° about the Y-axis with the nose skid as a pivot point, and landed upright on the landing gear.

In test 11, the yaw angle was set at 180° and the model was given a backward horizontal velocity of 10 ft/sec. In this test, the left rear main landing gear failed at the strut hinge point, and the drag brace member buckled.

Tests 12 to 24 were conducted on the hard-packed soil surface with horizontal velocities from 15 to 50 ft/sec and yaw angles from 0° to 15°. The vehicle proved quite stable on this surface, remaining upright for all test conditions.

Stability on Canvas Surface with Active Propulsion System

In the tests employing the propulsion system, there were three specific problems:

(1) The thrust vector was initially misalined with the model's center of gravity. The resulting torque was of sufficient magnitude to pitch the vehicle over on its heat shield when the model was not traveling at a horizontal velocity. After the proper thrust-vector alinement was achieved, the vehicle exhibited good pitch stability.

(2) The drop tower carriage imparted a tip-off torque to the model in the pitch plane upon release. The resultant angular pitch rate was

in the direction for pitching the nose of the model up. Thus, the horizontal component of the thrust imparted a backward velocity to the model. By the time the rear gear impacted, the pitch attitude had changed sufficiently that the backward horizontal velocity coupled with the horizontal component of the thrust vector was sufficient to pitch the model over on its heat shield, using the rear gear as a pivot point. This problem was corrected by moving the attachment bracket on the model so that it was directly above the model's center of gravity when the vehicle was trimmed for an attitude of -13°.

(3) At horizontal velocities of 20 ft/sec the trailing umbilical cable exerted an inertia force which caused the model to change its pitch and yaw attitudes prior to impact. This problem was overcome by accelerating the cable to a horizontal velocity equal to that of the model.

All tests in which one of these three problems occurred were rerun after the conditions were corrected.

Two of these problems are inherent to the model program only. However, the alinement of the thrust vector through the center of gravity is a problem in the prototype vehicle. The thrust vector must pass through the center of gravity within close limits ($\pm 1/2$ inch) or the vehicle will acquire undesirable motion, such as pitching over on the heat shield or rolling off the landing gear. However, the alinement of the thrust vector for the prototype vehicle should be less sensitive since it will be used in conjunction with a parachute and the parachute will be attached such that the parachute line loads will produce a torque to oppose any torque produced by a thrust vector misalinement.

The propulsion system's function was to attenuate the vertical component of velocity. The thrust-time relationship was obtained from the nozzle pressure-time trace. The velocity and distance-traveled time relationships were derived by direct integration of Newton's second law. Since the total drop height of the vehicle was known, the method of determining the velocity and distance traveled as a function of time is accurate, providing that the time required to travel the total distance analytically is equal to the total time to impact derived from the accelerometer data. The time required to travel the drop distance as determined analytically was compared to the total time to impact as derived from the accelerometer data. This comparison was made with favorable results on all tests in which the propulsion system was used. The vehicle motion during rocket firing, with combinations of present errors in the pitch angle of $\pm 5^{\circ}$ and yaw angles up to 15° and with horizontal velocities up to a simulated 30 ft/sec, was satisfactory. The vertical component of velocity at impact ranged from a simulated 5 to 10.5 ft/sec. This range of velocities was due to deviations in the sequencer and in the magnitude of the thrust.

Accelerations

Acceleration histories were recorded by means of accelerometers installed on the three major axes of the vehicle and in the direction of the thrust vector. Table I presents a summary of test results, including the vertical and horizontal velocities at impact, the model slideout distance, the average coefficient of friction for the main landing gear, the peak impact accelerations along the principal axes of the vehicle, and comments on the vehicle's stability. The range of impact accelerations for test conditions with and without the propulsion system was very comparable. Although tumbling and end-over-end flipping occurred, the accelerations encountered were relatively low and were well below the level of human endurance.

The maximum accelerations were recorded along the Y-axis. These accelerations ranged from 1.38g to 7.4g, with the higher values recorded during testing on the hard-packed soil surface without the propulsion system. These higher accelerations may be attributed to the fact that the apparent weight of the vehicle during sustainer phase thrusting is only one-half the real weight without the propulsion system and the sod attenuated more of the impact shock than the other landing surfaces.

No attempt was made to change the roll position from 0° during these tests, and the accelerations measured along the X-axis of the vehicle were negligible. The X-axis accelerations shown in table I were insignificant in magnitude and can be attributed to the irregularity of the landing surfaces, which caused the model to bounce and tip.

The accelerations recorded along the Z-axis were, likewise, small, ranging from a minimum of -0.24g to a maximum of 3.65g, which occurred during vehicle tumbling. These accelerations are proportional to vehicle pitch attitude, landing gear drag, and bouncing of the model about its pitch axis. It should be noted that in the test in which the gear failed, accelerations were approximately the same as those in the preceding test and the backward horizontal velocity caused the gear failure.

Coefficients of Frictions

For purposes of comparison, the average coefficient of friction for each test was calculated by the same method as that used in McDonnell's 1/4-scale model test report TR 052-042.10. This method arrives at a coefficient of friction by assuming that all horizontal energy is dissipated only by friction forces. It is derived by dividing the square of the horizontal velocity by twice the acceleration of gravity multiplied by the slide-out distance. This equation is not entirely valid because some of the horizontal energy is dissipated by the skids' either riding over or shearing the impact indentations in the landing surface. Although there is some fallacy in this equation, it is the best method available without more complex instrumentation. The average coefficients of friction are plotted in figure 9. The band between 0.4 and 0.6 represents values obtained with the load cell method. All tagged points are for tests which did not use the cold gas system. All of these points are higher than the band values, which indicates that the coefficient of restitution and surface irregularities affected these tests to a much greater extent than the test made with the propulsion system.

Table I shows the slide-out distances used in calculating the coefficients of friction for each run. On tests 3 and 12, which were made on sod and soil without the propulsion system, slide distances of about 1 foot were recorded. These tests were made with horizontal velocities of 15 ft/sec and vertical velocities of 10 ft/sec. While under the same landing conditions, a slide-out distance of $7\frac{1}{3}$ feet was recorded on test 26, with the active propulsion system. However, the coefficients of friction for the three surfaces are comparable. The difference in slide-out distance with the propulsion system is attributed to the lower drag force on the skids as a result of the reduction in normal force because of the sustainer thrust.

In test 33, where the vehicle's pitch attitude was increased to -18° nose down, the slide-out distance for the model increased to 11 feet. This increase was caused by the horizontal component of the propulsion system thrust vector attributed to the change in attitude.

Surface Erosion

The results of the test in which the propulsion system was exhausted directly upon the compacted soil surface were of interest as qualitative data only. It would not be correct to say that this soil was entirely representative of either a prepared or an unprepared landing surface that could be used for a spacecraft recovery. The exhaust plume of the sustain phase of the cold-gas system blasted a hole in the surface approximately 30 inches in diameter and 8 inches deep when the model had no horizontal velocity (fig. 10).

The model was then given a horizontal velocity of 3.62 ft/sec, and the propulsion system was again activated at sustainer level. Two ruts approximately 8 inches wide and 2 inches deep were made (fig. 11). These preliminary data indicate that if a landing rocket recovery system is used, then soil erosion caused by rocket plume will require additional study.

CONCLUSIONS

Tests were conducted to determine the feasibility of using the Para-Sail/landing rocket combination as the landing system on the present Gemini spacecraft. A $\frac{1}{3}$-scale Gemini spacecraft with a cold-gas deceleration system and a tricycle skid landing gear was used. From the results of the tests, the following conclusions may be drawn:

(1) By using directional control furnished by the Para-Sail and with the low vertical rate of descent made possible by the use of landing rockets, accelerations will be small, with magnitudes in the order of 10g or less. During these tests, the maximum accelerations recorded were 7.4g (Y-axis), 3.1g (X-axis), and 1.62g (Z-axis).

(2) The present Gemini landing gear will operate satisfactorily on a smooth, prepared surface; however, tumbling is imminent on sod or on other irregular surfaces where penetration can occur, causing the landing gear to trip.

(3) The present Gemini landing gear is not designed for extreme yaw conditions. At 180° yaw (backward) landing, the gear will probably fail; however, accelerations will be low. It is not feasible to redesign the landing gear to compensate for this handicap because of the spacecraft's tendency to turn over on its heat shield when the landing rockets are thrusting.

(4) Proper thruster alinement with the vehicle's center of gravity is critical. Also, wide variations in vehicle weight and attitudes cannot be tolerated from the standpoint of impact accelerations and vehicle stability.

(5) Tests are required where a parachute is used in conjunction with the landing rockets to determine the drag force and vehicle stability as a function of time during rocket firing.

(6) Under certain landing conditions, soil erosion caused by the propulsion system may create ruts large enough to cause gear trippage. With the data presently available it appears that erosion could be a problem.

TABLE I.- LANDING IMPACT AND STABILITY TEST OF 1/3-SCALE GEMINI MODEL

(a) Test conducted on St. Augustine sod; propulsion system not used

Test No.	Horizontal velocity, ft/sec		Pitch angle, deg	Yaw angle, deg	Slide-out distance		Average coefficient of friction		Peak impact acceleration, g			Vertical impact velocity, ft/sec		Stability
	Actual	Full scale			Right, ft	Left, ft	Right	Left	Y	X	Z	Actual	Full scale	
1	0	0	-13	0	0	0	-	-	-	-	-	5.77	10	Good
2	0	0	-13	0	0	0	-	-	4.0	-	0.3	5.77	10	Good
3	8.65	15	-13	0	1.00	1.00	1.16	1.16	3.0	0.2	1.0	5.77	10	Good
4	8.65	15	-13	5	0.90	0.92	1.31	1.28	5.1	0.4	1.0	5.77	10	Good
5	8.65	15	-13	10	0.90	0.92	1.31	1.28	5.8	2.3	1.1	5.77	10	Good
6	8.65	15	-13	15	0.88	0.90	1.34	1.30	6.3	0.5	1.1	5.77	10	Good
7	17.30	30	-13	0	6.00	6.00	0.78	0.78	7.2	0.3	1.4	5.77	10	Good
8	17.30	30	-13	5	-	-	-	-	6.2	0.2	1.4	5.77	10	Tumbled
9	17.30	30	-13	10	-	-	-	-	7.4	0.7	1.5	5.77	10	Tumbled
10	28.8	50	-13	0	-	-	-	-	6.0	0.4	1.6	5.77	10	360° flip
11	5.78	10	-13	180	-	-	-	-	4.0	0.2	0.6	5.77	10	Damaged both main landing gear

TABLE I.- LANDING IMPACT AND STABILITY TEST OF 1/3-SCALE GEMINI MODEL - Continued

(b) Test conducted on compacted earth; propulsion system not used

Test No.	Horizontal velocity, ft/sec		Pitch angle, deg	Yaw angle, deg	Slide-out distance		Average coefficient of friction		Peak impact acceleration, g			Vertical impact velocity, ft/sec		Stability
	Actual	Full scale			Right, ft	Left, ft	Right	Left	Y	X	Z	Actual	Full scale	
12	8.65	15	-13	0	1.04	1.04	1.12	1.12	5.50	2.30	1.00	5.77	10	Good
13	0	0	-13	0	0	0	-	-	5.50	0.70	1.00	5.77	10	Good
14	8.65	15	-13	5	0.92	0.96	1.27	1.21	5.70	0.80	1.40	5.77	10	Good
15	8.65	15	-13	10	0.92	0.96	1.27	1.21	6.30	2.20	1.10	5.77	10	Good
16	8.65	15	-13	10	0.71	0.73	1.64	1.60	6.30	3.10	1.00	5.77	10	Good
17	17.30	30	-13	0	6.29	6.59	.74	.71	5.90	2.10	1.20	5.77	10	Good
18	17.30	30	-13	5	6.59	7.13	.71	.66	6.20	1.00	1.20	5.77	10	Good
19	17.30	30	-13	10	6.17	7.00	.75	.67	6.16	0.18	1.12	5.77	10	Good
20	17.30	30	-13	15	7.00	7.67	.67	.61	5.90	0.08	1.26	5.77	10	Good
21	28.80	50	-13	0	18.38	18.68	.76	.69	5.35	0.14	0.60	5.77	10	Good
22	28.80	50	-13	5	18.91	19.17	.68	.67	6.80	0.28	1.50	5.77	10	Good
23	28.80	50	-13	10	21.00	21.82	.62	.59	5.75	-	1.33	5.77	10	Good
24	28.80	50	-13	15	20.70	21.60	.63	.60	5.10	0.06	1.20	5.77	10	Good

TABLE I.- LANDING IMPACT AND STABILITY TEST OF 1/3-SCALE GEMINI MODEL - Continued

(c) Test conducted on canvas; propulsion system used

Test No.	Horizontal velocity, ft/sec		Pitch angle, deg	Yaw angle, deg	Slide-out distance		Average coefficient of friction		Peak impact acceleration, g			Vertical impact velocity, ft/sec		Stability
	Actual	Full scale			Right, ft	Left, ft	Right	Left	Y	X	Z	Actual	Full scale	
25	0	0	-13	0	-	-	-	-	3.76	0.80	1.11	5.95	10.30	Good
26	8.65	15	-13	0	7.33	7.33	0.318	0.318	3.49	0.00	1.22	4.72	8.20	Good
27	8.65	15	-13	5	8.33	8.17	0.280	0.289	2.42	0.00	0.61	5.29	9.15	Good
28	8.65	15	-13	10	6.50	6.58	0.359	0.400	3.49	0.00	1.45	4.58	7.94	Good
29	8.65	15	-13	15	-	-	-	-	3.49	1.12	1.12	4.85	8.40	Good
30	0	0	-18	0	0.42	0.42	-	-	7.00	1.13	1.33	3.74	6.50	Model translated 9 in. forward; stable
31	8.65	15	-18	0	10.92	11.17	0.214	0.300	2.84	2.36	1.62	4.83	8.35	Good (model appeared yawed)
32	8.65	15	-18	5	-	-	-	-	3.22	1.39	1.62	4.28	7.40	Good
33	8.65	15	-18	10	11.17	11.08	0.300	0.210	4.35	-	1.62			Good
34	8.65	15	-18	15	10.58	10.25	0.220	0.227	3.77	1.85	1.22	4.32	7.32	Good
35	8.65	15	- 8	0	6.00	6.42	0.388	0.363	1.57	0.00	1.22	5.05	8.75	Good
36	8.65	15	- 8	15	6.25	6.67	0.373	0.350	3.67	1.93	0.81	4.85	8.40	Good
37	8.65	15	-13	0	-	-	-	-	4.20	1.85	1.42	4.42	7.66	Good
38	17.30	30	-13	0	-	-	-	-	5.10	-	3.65	4.50	7.80	Cable fouled R/H MLG causing model to tumble 360°
39	17.30	30	-13	0	13.25	14.25	0.704	0.655	4.32	0.93	1.62	5.62	9.75	Good
40	11.52	20	-13	0	11.50	11.25	0.360	0.368	2.69	1.85	1.45	3.82	6.60	Good

TABLE I.- LANDING IMPACT AND STABILITY TEST OF 1/3-SCALE GEMINI MODEL - Concluded

(c) Test conducted on canvas; propulsion system used - concluded

Test No.	Horizontal velocity, ft/sec		Pitch angle, deg	Yaw angle, deg	Slide-out distance		Average coefficient of friction		Peak impact acceleration, g			Vertical impact velocity, ft/sec		Stability
	Actual	Full scale			Right, ft	Left, ft	Right	Left	Y	X	Z	Actual	Full scale	
41	14.20	25	-13	0	13.75	13.67	0.456	0.456	5.36	0.00	0.94	3.31	5.72	Good
42	12.95	22.5	-13	0	10.17	11.00	0.514	0.473	4.94	0.00	1.21	4.20	7.30	Good
43	17.30	30	-18	0	16.25	18.42	0.574	0.506	3.22	0.95	1.11			Good
44	17.30	30	-8	0	13.42	14.25	0.695	0.655	3.22	0.00	1.55			Good
45	17.30	30	-13	15	14.00	15.00	0.666	0.623	5.66	0.00	1.33			Good
46	17.30	30	-13	15	15.50	16.00	0.601	0.584	3.31	1.01	1.33			Good
47	17.3	30	-13	15	13.92	15.58	0.67	0.60	4.54	1.01	1.55			Good
48	17.3	30	-13	5	12.83	14.33	0.72	0.65	1.38	0.00	1.30			Good
49	17.3	30	-8	15	14.83	15.17	0.63	0.62	3.41	1.01	1.33			Good
50	17.3	30	-18	15	18.58	19.25	0.50	0.48	3.24	2.02	1.55			Good

NASA-S-65-4279

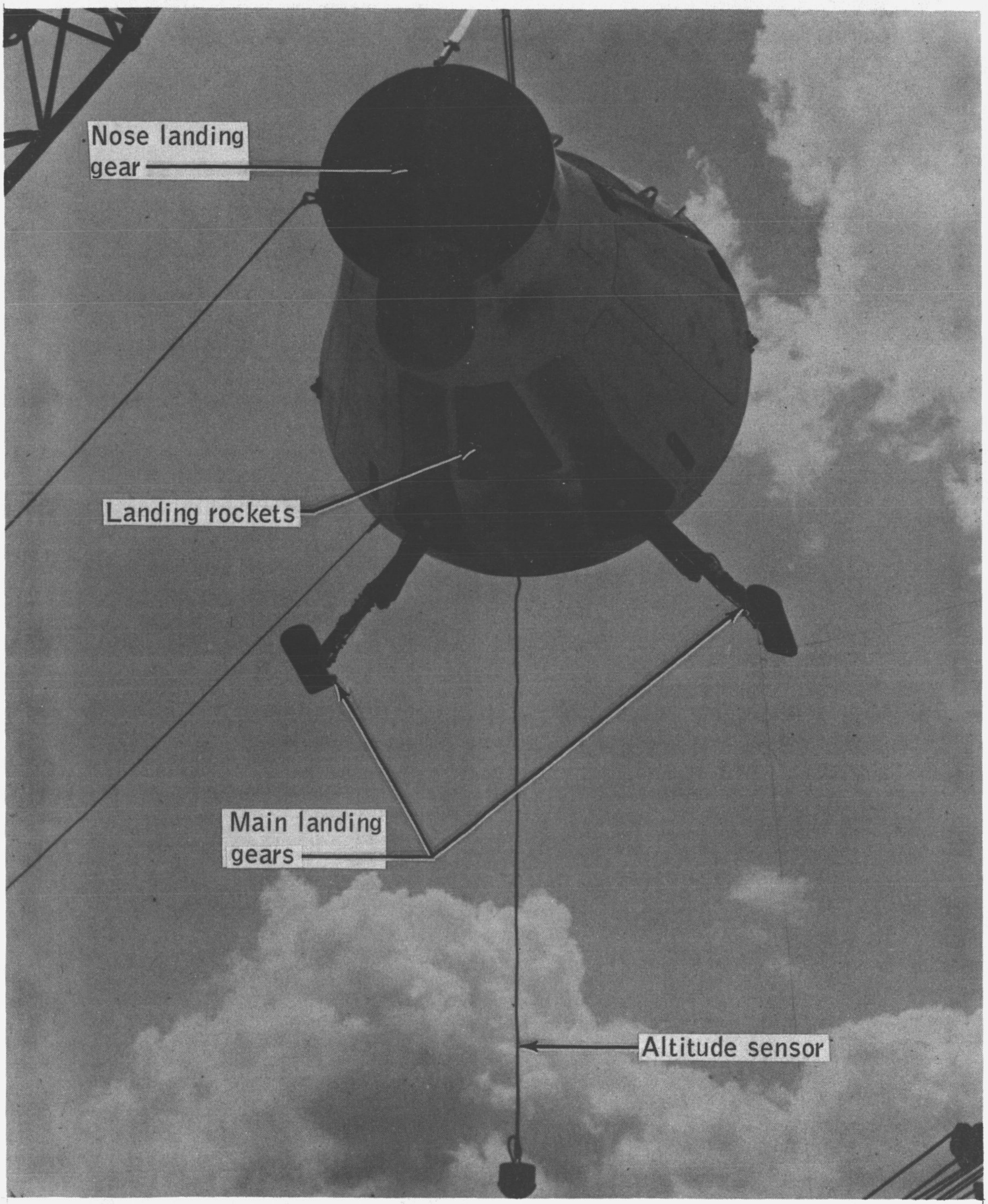

(a) Complete full-scale system
Figure 1. - Landing system

NASA-S-65-4287

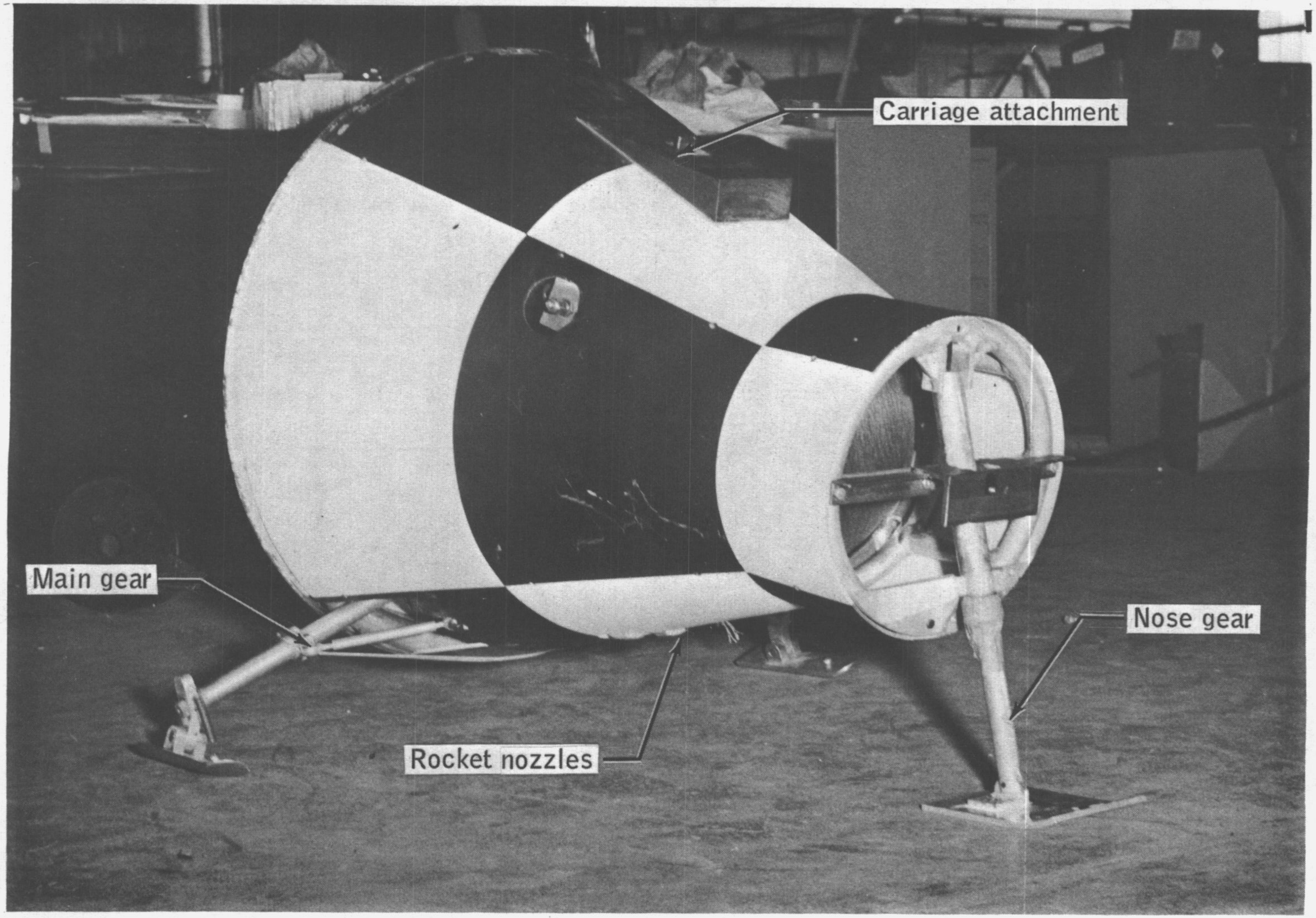

(b) 1/3-scale test model
Figure 1. - Landing system

NASA-S-65-4277

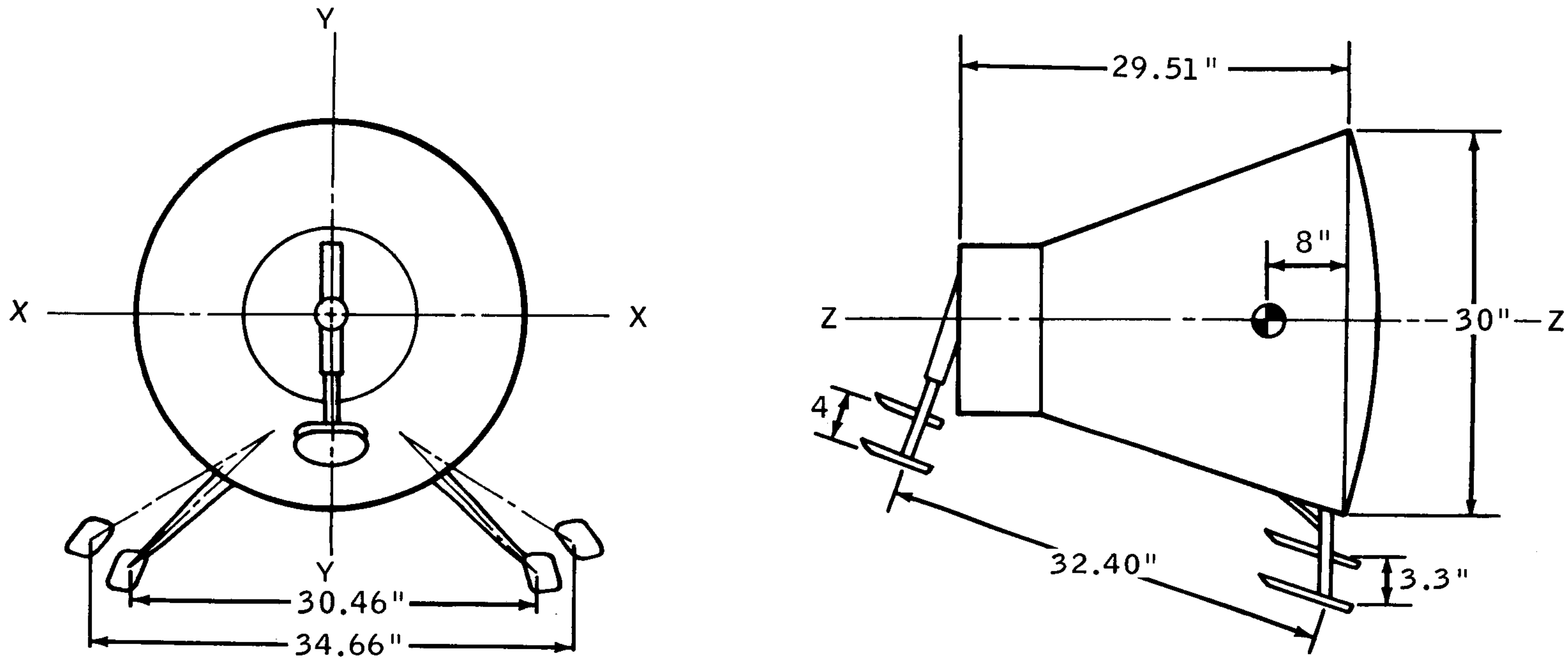

	Model	Scale factor	Full scale
Weight	176.6 lb	3^3	4768.2 lb
Inertia, X-X (yaw)	4.18 slugs/ft^2	3^5	1016 slugs/ft^2
Inertia, Y-Y (pitch)	4.35 slugs/ft^2	3^5	1058 slugs/ft^2
Inertia, Z-Z (roll)	3.15 slugs/ft^2	3^5	766 slugs/ft^2

Figure 2. - Model dimensions, center-of-gravity location, weight, and inertias

NASA-S-65-4280

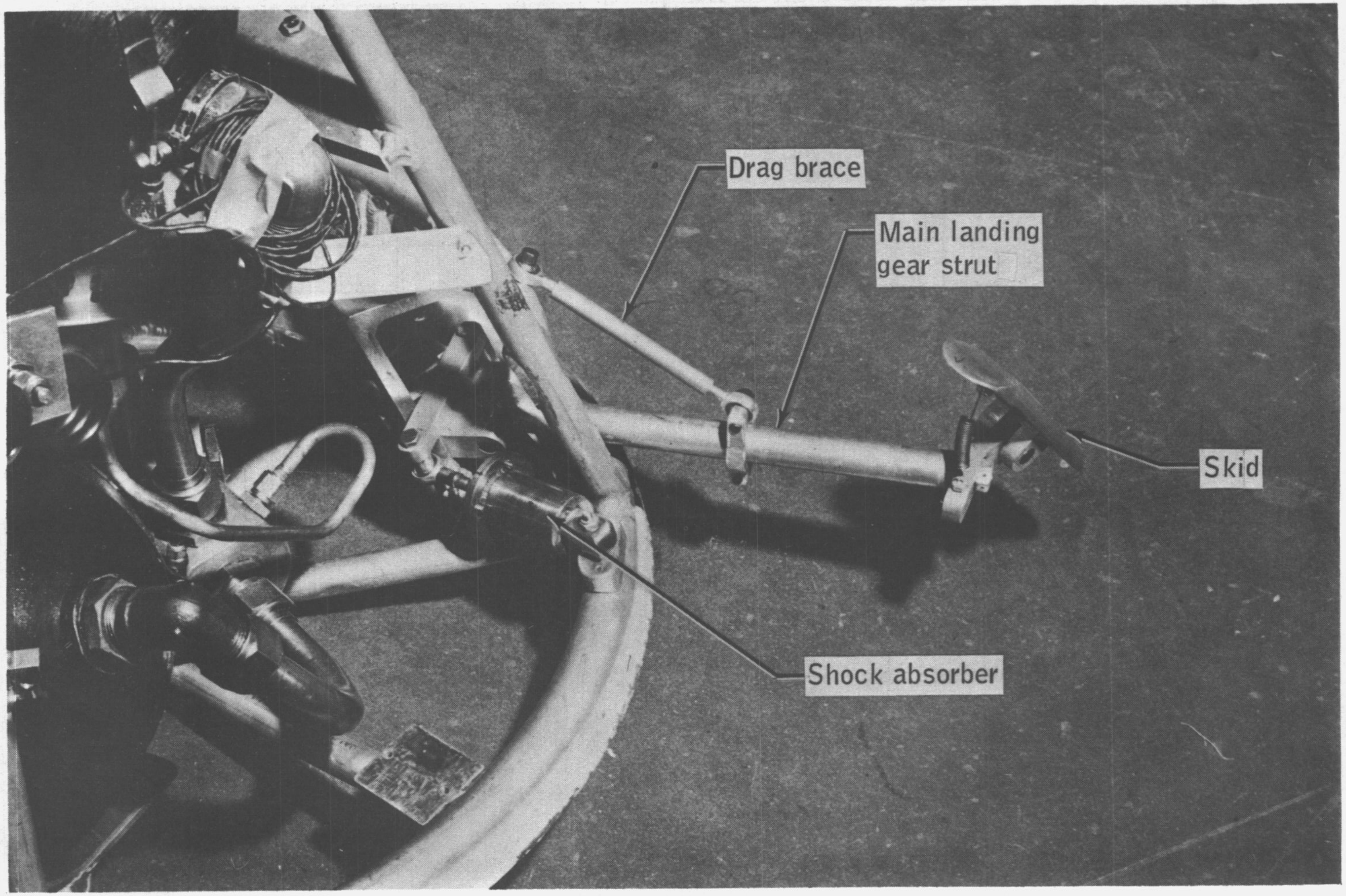

Figure 3. - Main landing gear detail

NASA-S-65-4284

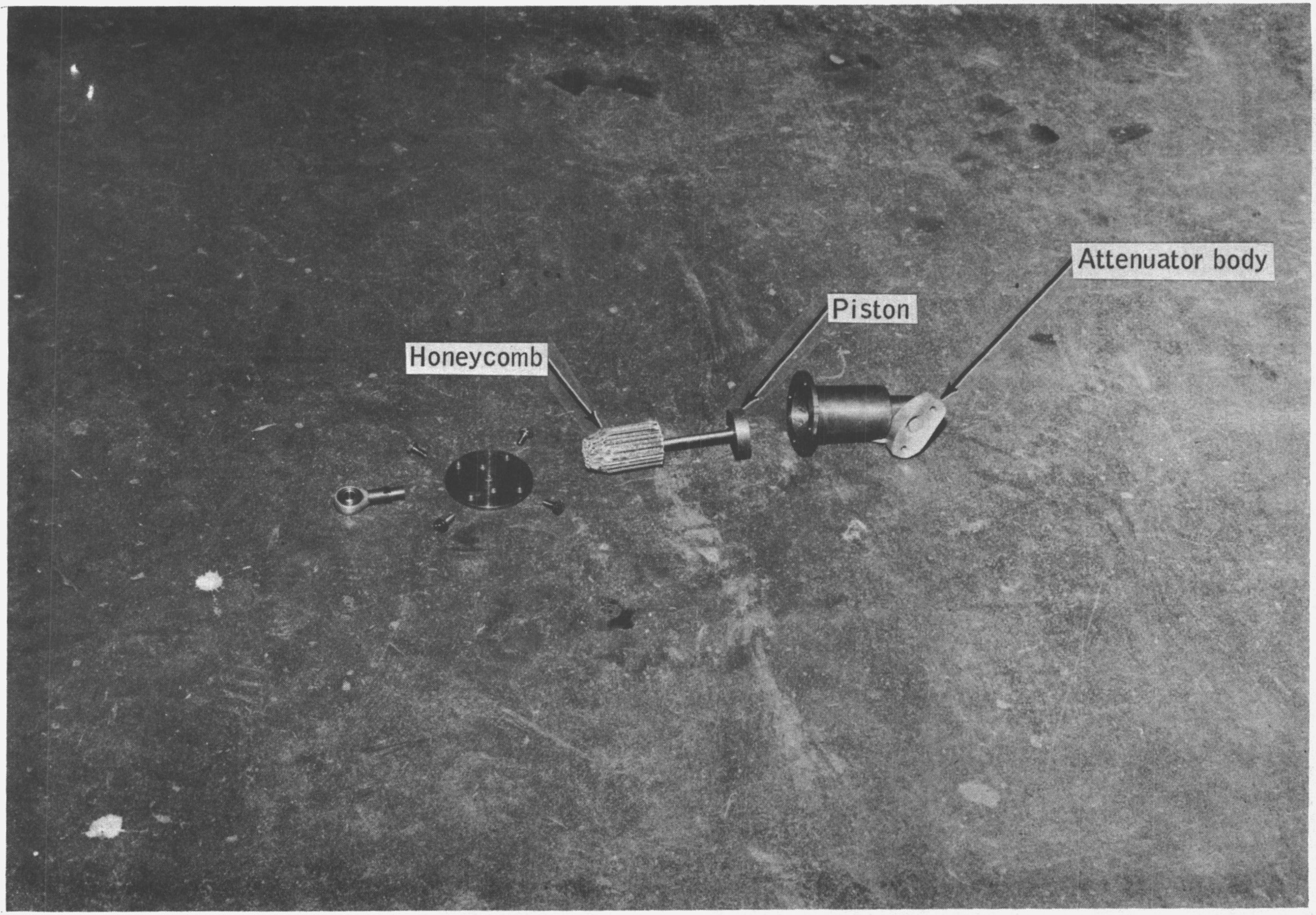

Figure 4. - Main landing gear shock attenuator

NASA-S-65-4283

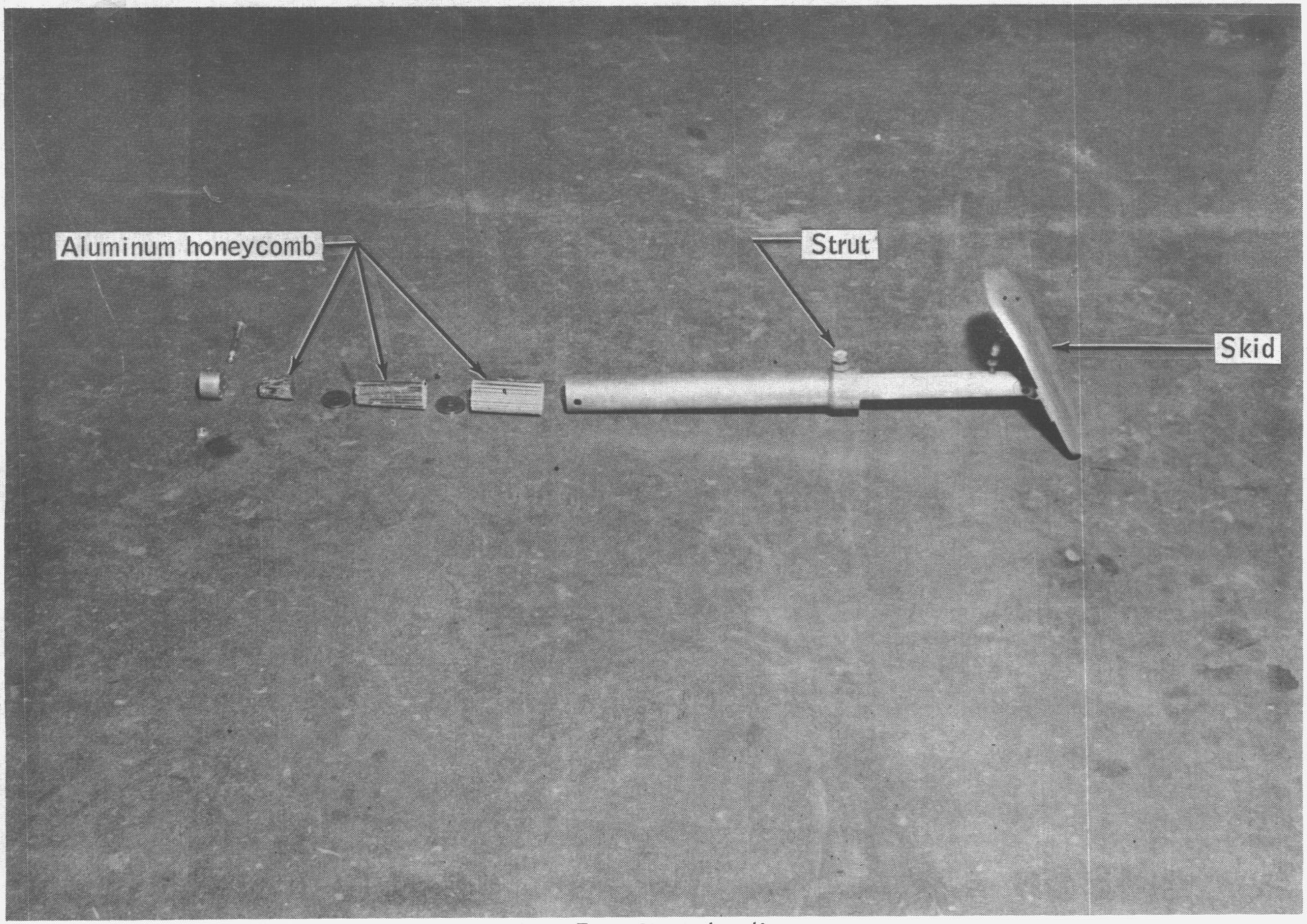

Figure 5. - Nose landing gear

NASA-S-65-4286

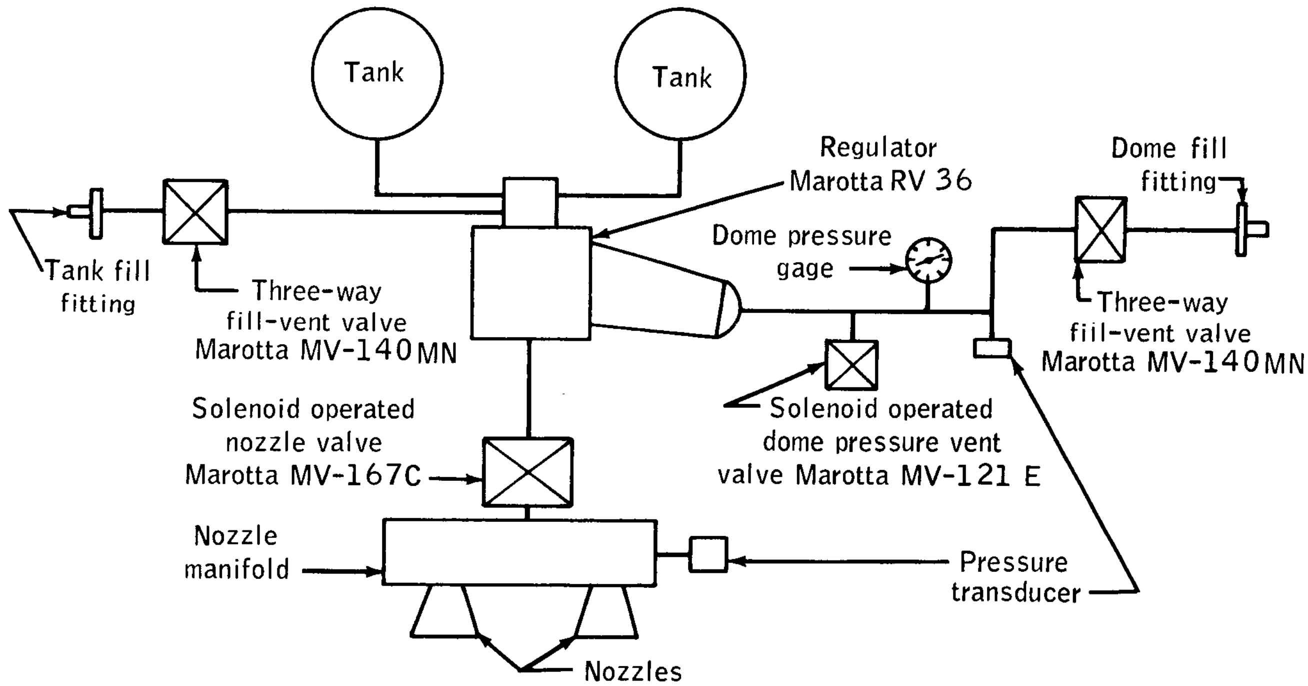

Figure 6. - Schematic of propulsion system (1/3-scale Gemini)

NASA-S-65-4278

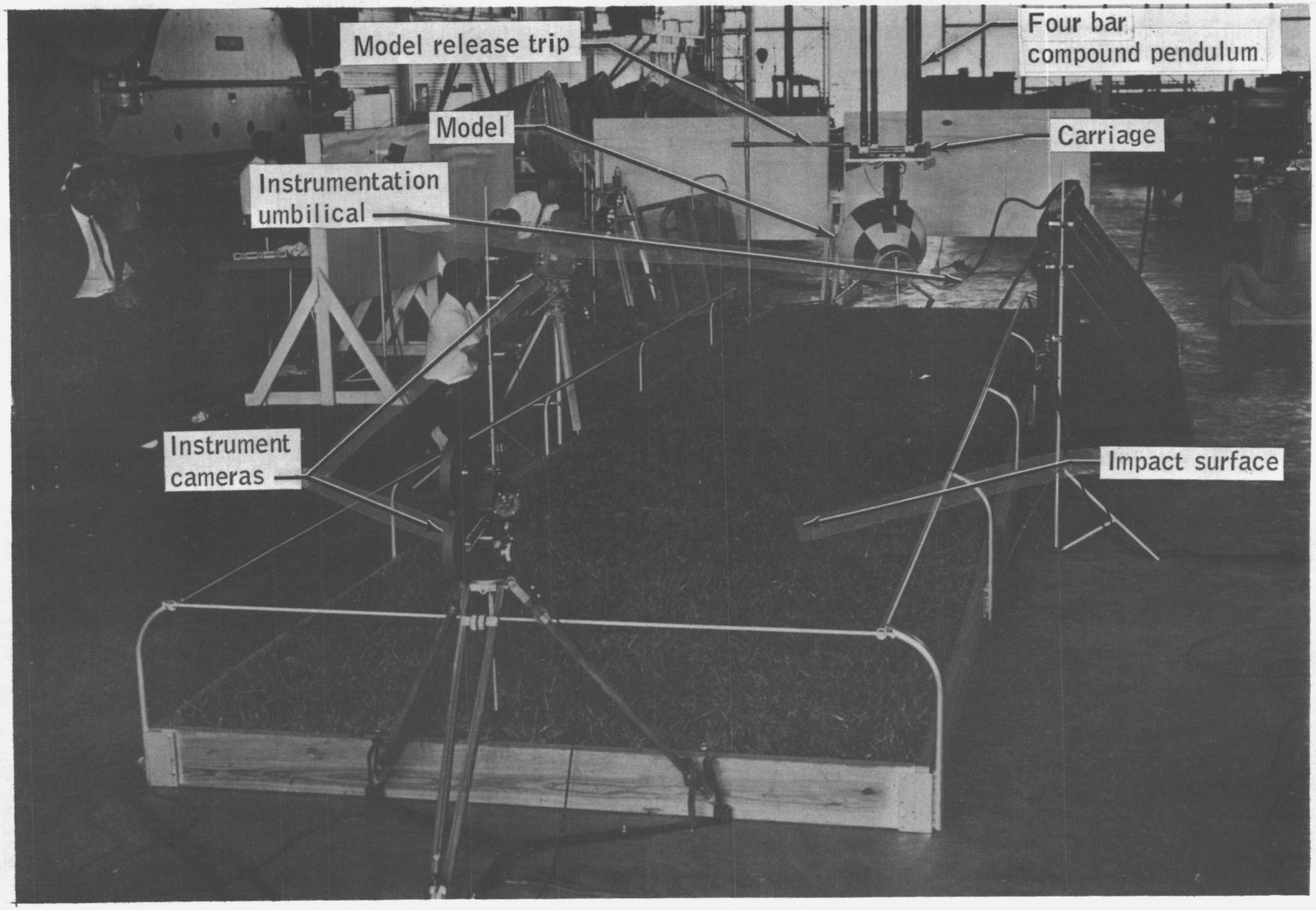

Figure 7. - Test facility

NASA-S-65-4288

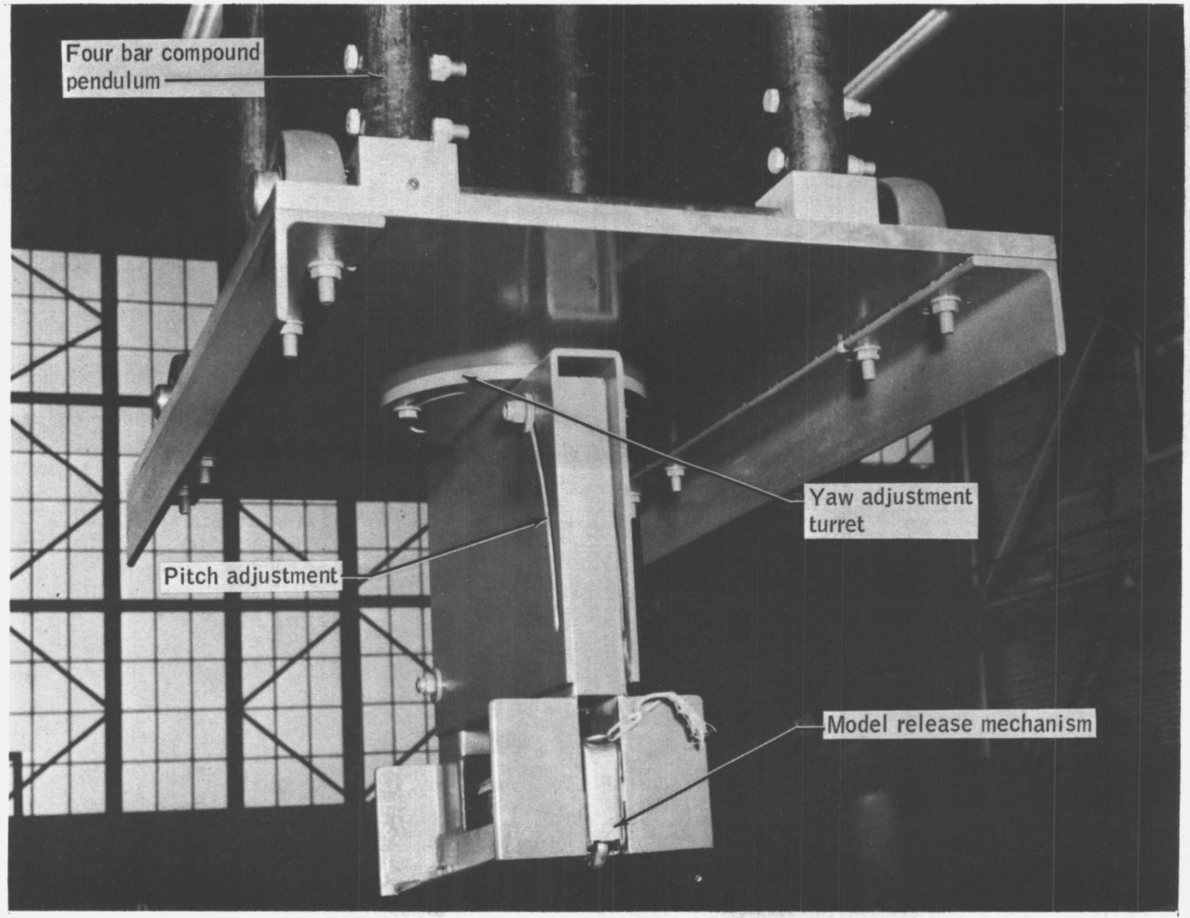

Figure 8. - Drop carriage

NASA-S-65-4285

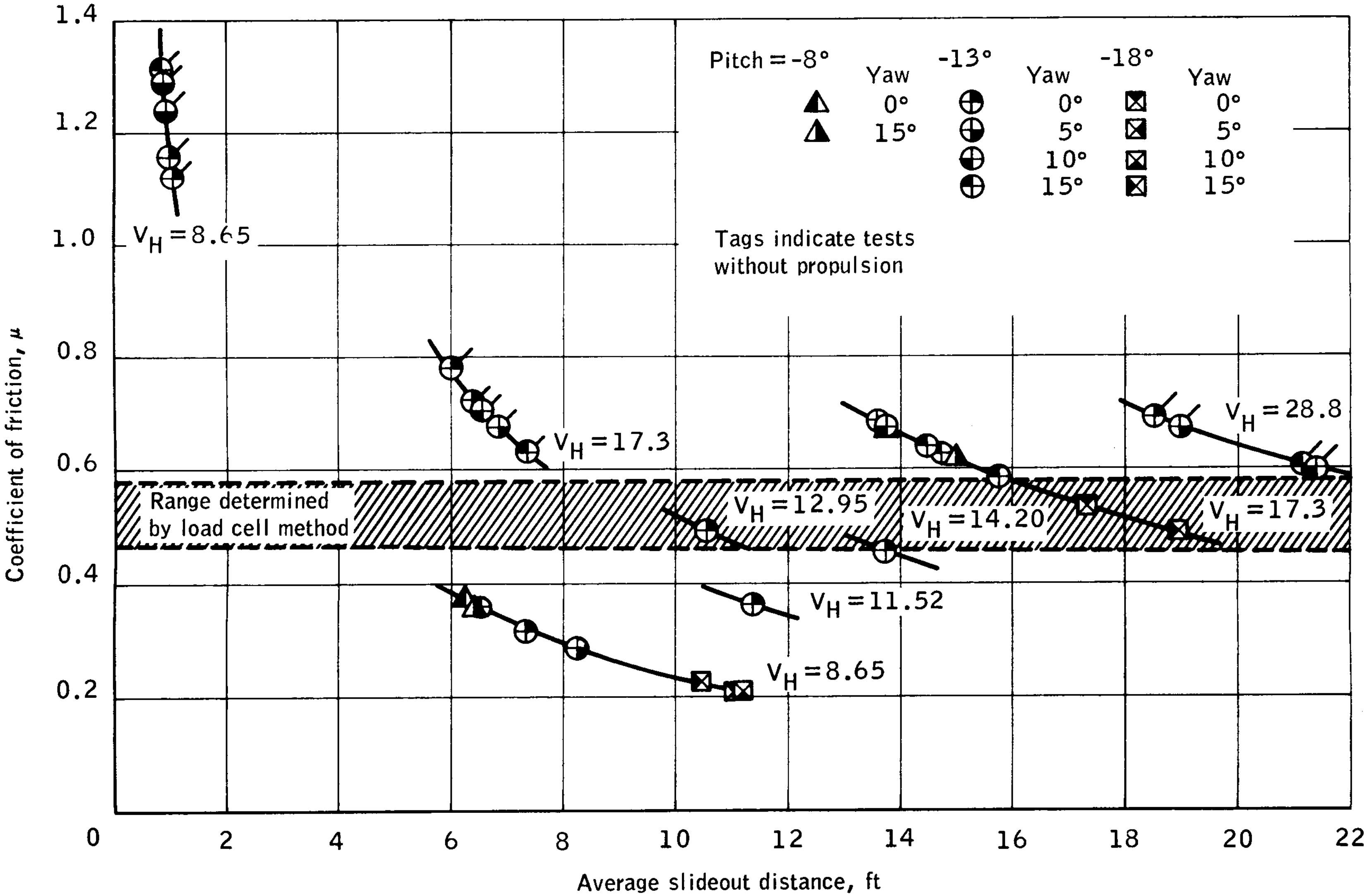

Figure 9. - Coefficients of friction

NASA-S-65-4282

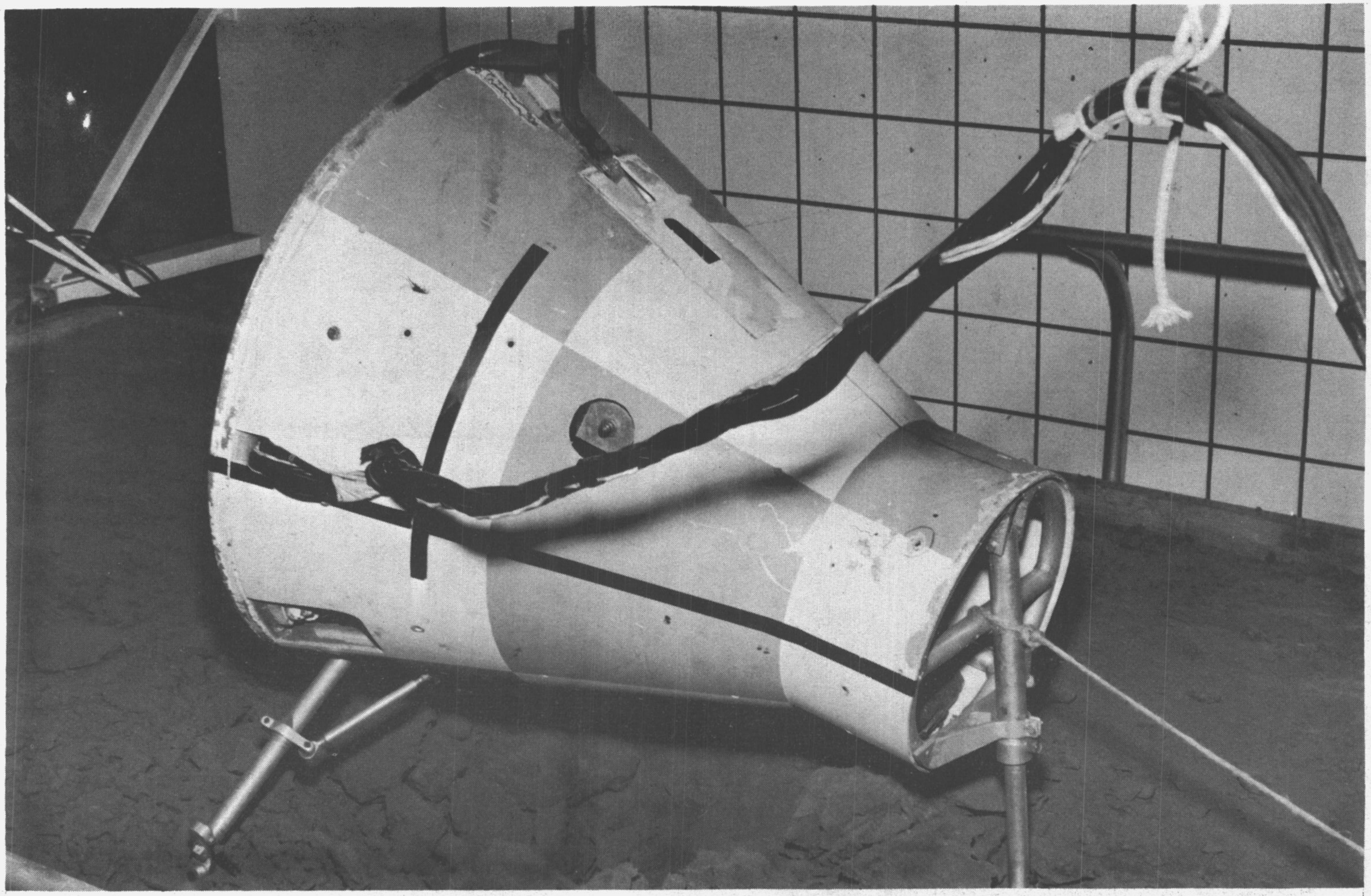

Figure 10. - Soil erosion caused by model at 0 horizontal velocity

NASA-S-65-4281

Figure 11. - Soil erosion caused by model at 3.5 ft/sec horizontal velocity